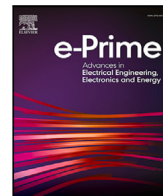




Contents lists available at ScienceDirect

# e-Prime - Advances in Electrical Engineering, Electronics and Energy

journal homepage: [www.elsevier.com/locate/prime](http://www.elsevier.com/locate/prime)

## Beyond lithium: A comprehensive use-case-analysis of sodium-ion-battery technology in battery electric vehicles

Jan Koloch <sup>1</sup>\*, Jakob Schneider <sup>2</sup>, Moritz Seidenfus <sup>2</sup>, Markus Lienkamp

<sup>1</sup>Technical University of Munich (TUM), Germany

<sup>2</sup>School of Engineering & Design, Institute of Automotive Technology, Boltzmannstraße 15, 85748 Garching bei München, Germany

### ARTICLE INFO

#### Keywords:

Sodium-ion batteries  
Battery electric vehicles  
Techno-economic analysis  
Vehicle system design  
Cell chemistry comparison

### ABSTRACT

Passenger vehicle fleets must incorporate more battery electric vehicles to achieve climate neutrality goals. With the need for affordable electric vehicles to lower barriers to customer adoption, innovations in battery technology are necessary. Sodium-ion batteries (SIBs) represent an emerging technology offering potential advantages, particularly regarding battery cost reduction. Therefore, this study conducts a techno-economic analysis of SIBs in electric vehicles. For this purpose, a vehicle simulation was developed and supplemented with a cost model. Results show that SIBs demonstrate the lowest cost per kilometer compared to NMC and LFP battery chemistries, with up to 21.8% lower costs per kilometer when switching from NMC to SIB. While vehicles with SIBs exhibit slightly lower maximum ranges than reference batteries, this difference is small. Results additionally demonstrate that implementing maximum battery capacity in the SIB configuration proves economically advantageous. This economic advantage is particularly pronounced when low-cost home charging options are available. The main disadvantage of SIB equipped electric vehicles lies in packaging constraints due to lower volumetric energy density, which limits the feasibility of vehicles with high battery capacities. According to the analysis framework, therefore, only electric vehicles with a battery capacity up to 59 kWh can be realized. Sensitivity analysis of SIB cell properties reveals the small influence of gravimetric energy density and the significant impact of specific battery costs on cost per kilometer. A comparative analysis of electric vehicles with low battery capacity using NMC and LFP cell chemistries versus maximum utilization of SIB capacity demonstrates that SIBs achieve lower costs per kilometer while enabling higher maximum range, thus presenting a promising alternative to lithium-ion batteries. A comparative analysis of electric vehicles with low battery capacity using NMC and LFP cell chemistries versus maximum utilization of SIB capacity demonstrates that SIBs achieve 1 €/100 km lower costs per kilometer while enabling 64 km higher maximum range than NMC, thus presenting a promising alternative to lithium-ion batteries.

### 1. Introduction

In the Paris Agreement, the European Union (EU) committed to meeting the ambitious target of climate neutrality by 2050 to keep global warming below 2 °C and pursuing efforts to limit it to 1.5 °C [1, 2]. This implies climate-neutral transport by 2050, whereby transportation responsible for approximately one-quarter of the EU's energy-related greenhouse gas emissions is [1,3,4]. Stricter legislative requirements are being imposed to achieve the climate targets in the transport sector. These include, among others, the new Euro 7 emission standard for light- and heavy-duty vehicles in the EU, which aims to further reduce pollutant emissions from road transport [5,6]. The Euro 7 emission standard introduces new type-approval regulations, including stricter requirements than Euro 6, thereby creating additional incentives for original equipment manufacturers (OEMs) to transition

towards BEVs. For the first time, Euro 7 also establishes specific requirements for BEVs, considering the battery lifetime and state of health (SOH) indicators, making battery systems subject to increased legislative examination. Moreover, Euro 7 is regarded as the final step in the transition towards zero-emission vehicles, emphasizing the significance of BEVs and the continued need for research in this field [7]. Additionally, fleet emission limits and associated penalty payments for exceeding these limits provide further incentives for OEMs to advance BEV development [8].

The elevated investment of BEVs present a significant barrier to BEVs adoption [9]. Following König et al. [10] and Kumar and Alok [11], the acquisition price remains an important factor in purchasing decisions. Reducing investment costs increases customer acceptance and willingness to buy BEVs. Hereby, the battery system represents

\* Corresponding author at: School of Engineering & Design, Institute of Automotive Technology, Boltzmannstraße 15, 85748 Garching bei München, Germany.  
E-mail address: [jan.koloch@tum.de](mailto:jan.koloch@tum.de) (J. Koloch).

<https://doi.org/10.1016/j.prime.2025.100995>

Received 29 January 2025; Received in revised form 4 March 2025; Accepted 11 April 2025

Available online 25 April 2025

2772-6711/© 2025 The Authors. Published by Elsevier Ltd. This is an open access article under the CC BY license (<http://creativecommons.org/licenses/by/4.0/>).

the core element of electric vehicles, requiring particular attention in research and development [12]. Furthermore, vehicle range constitutes another crucial purchasing criterion [11]. According to Pamidimukkala et al. [9], while environmental friendliness and carbon dioxide emissions represent relevant factors for many customers, they play a subordinate role compared to purchase price. Therefore, it is essential for OEMs during the early development phase to target the decisive vehicle segments for their customer base and be aware of customer expectations regarding electric vehicles. LIBs are the dominant energy storage technology for BEVs due to their beneficial electrochemical storage properties [13]. However, this technology faces significant challenges, including cost-intensive raw materials with environmentally harmful extraction processes, potential lithium supply bottlenecks, and geopolitical dependencies in supply chains [14–16]. SIBs currently represent a heavily researched and promising alternative to LIBs [17–21]. The advantages of SIBs include environmental friendliness due to fewer critical raw materials, comparable electrochemical principles and production processes to LIBs, and its lower specific cost per kWh [22]. SIBs are considered promising for BEV applications, leading major battery manufacturers like CATL and Northvolt to focus their research and development efforts on this technology [23,24]. Also, Chinese electric vehicle manufacturers have already presented SIB-powered BEV concepts [25–27].

Therefore, SIBs demonstrate significant potential for deployment in electric vehicle applications. This provides the key motivation for this study, which aims to identify the ideal battery cell technology for electric vehicles based on economic efficiency. This analysis enables the determination of specific use-cases where SIBs offer the most promising implementation opportunities. In the following, battery cell technology assessments regarding vehicle-level properties are reviewed to establish this study's analytical framework.

Teichert et al. [28] and Schneider et al. [29,30] analyzed the implications of LIB cells for battery electric truck (BET) applications. Teichert et al. [28] demonstrate the techno-economic selection of LIB cells for battery-electric long-haul trucks. Their method determines the required cell price to achieve cost parity with diesel trucks based on cell datasheet characteristics. Schneider et al. [29] evaluate the choice of battery size and chemistry regarding feasibility and cost-effectiveness for BETs using NMC and LFP battery cell chemistries. Furthermore, Schneider et al. [30] analyze the influence of LIB size and cell chemistry on the life-cycle carbon emissions of BETs. These studies focus on a different application case than targeted in the present study. However, they establish valuable analytical frameworks for assessing battery cell properties at the vehicle level.

Link et al. [31] present a high-level techno-economic framework for LIB cell selection based on cost parity pricing for mobile applications, including electric vehicles. Their results demonstrate that cell chemistries, rather than cell formats, are decisive for determining the most suitable applications. Additionally, their findings emphasize the importance of tailored cell selection strategies for decision-makers to optimize performance and cost-effectiveness across different applications.

Rudola et al. [22] analyzed the opportunities in the application of SIBs on BEVs. Their analysis addresses raw material prices, energy densities, and cycle lives of SIBs while examining their influence on the driving range. The study compares NMC, nickel cobalt aluminum oxide (NCA), LFP, and SIB technologies for electric vehicle applications. Results indicate that SIBs show similarities to LFP cell chemistry. A transition from LFP to SIB is expected to yield up to 19% savings in electric vehicle battery pack costs. When switching from LFP batteries to SIBs in electric vehicles, the maximum driving ranges are projected to be similar or slightly inferior to LFP. The study concludes that considering SIB chemistries' sustainability and cost advantages compared to LFP-based batteries, SIB-based electric vehicles show strong potential for moderate-range applications. While their analysis provides detailed

Table 1

Literature overview of battery technology assessments regarding vehicle-level properties.

Assessment aspects	LIB	SIB
Cost parity prices	[28–31]	–
Influence charging prices	[28,29]	–
Driving ranges	[22,32]	[22,32]
Vehicle prices	[22,32]	[22,32]
Vehicle segments	[32]	–

insights into driving range implications, it does not address comprehensive economic and vehicle-related implications. Furthermore, the study does not examine which specific vehicle segments would be most suitable for SIB implementation.

Hasselwander et al. [32] developed a techno-economic model to evaluate the impact of different battery technologies, including SIBs, for BEV applications. Their research employed a bottom-up systematic approach to assess various cell chemistries' technical and economic viability and their influence on vehicle range and total cost. The results demonstrate that implementing LFP or SIBs could substantially reduce electric vehicle costs to achieve price parity with conventional combustion vehicles. Despite their lower energy densities, these chemistries achieve acceptable driving ranges through cell-to-pack technology implementation, which is particularly advantageous due to their inherent safety characteristics. The study concludes that SIBs, similar to LFP batteries, show strong potential for future low-cost vehicle applications based on their comparable properties. While their analysis provides comprehensive insights into various future cell chemistries' effects on vehicle prices and ranges, SIBs are not the primary focus of their investigation. Furthermore, the study does not specifically address the optimal use-cases for SIB implementation in electric vehicles. A comprehensive overview of existing research regarding the implications of battery technologies on vehicle-level properties is presented in Table 1.

As shown in the state of the art, the implications of novel battery technologies, such as SIBs, for electric vehicles have only been partially examined in the literature. While individual studies address certain characteristics, holistic research quantifying and analyzing the comprehensive impact of SIBs on electric vehicles regarding cost-relevant and vehicle-specific properties is still missing. Furthermore, there is no systematic evaluation of which vehicle concepts would benefit most from SIB technology. Also, prior research fails to consider the implications of charging prices and does not provide insights into the impact of sensitivities of SIB characteristics. Moreover, cost parity prices for SIBs have not yet been presented in the literature. Such comprehensive analysis would be crucial to systematically evaluate the potential of SIB technology for different electric vehicle segments.

Therefore, this study addresses the technological and economic viability of SIBs as an alternative to LIBs in electric vehicle applications. The central research question focuses on determining whether and under which conditions SIB technology provides economic advantages over established LIB technology across different vehicle segments. The analysis is constrained to key battery parameters using a reference vehicle approach. The study thus provides insights into the economic vehicle-level effects of SIB technology adoption. Based on the research gaps, the main contributions of this paper can be summarized as follows:

- **Vehicle-level technology assessment**  
Analysis of fundamental relationships between SIB technology and electric vehicles, focusing on battery capacity sizing, trip ranges, and charging costs compared to LIBs.
- **Sensitivity analysis of cell properties on vehicle-level parameters**  
Quantification of how changes in sodium-ion cell characteristics affect vehicle-level performance and specifications, enabling evaluation of technological uncertainties in vehicle development through detailed sensitivity studies.

The findings of this study provide valuable insights for automotive research and development departments to evaluate and quantify the potential of SIBs, particularly from a cost perspective, for future electric vehicle powertrains. The methodology enables systematic analysis of technical feasibility and economic viability in the context of automotive requirements and constraints.

The paper is structured as follows: Section 2 outlines the methodology for the use-case analysis, including the simulation approach and the developed cost model. Section 3 shows the results, focusing on four main aspects: First, the analyzed cost-optimal relationships are presented between cell technology, battery capacity, and trip range. Second, the influence of home and external charging on battery-related costs is investigated. Third, a sensitivity analysis of sodium-ion cell properties on vehicle-relevant characteristics is conducted. Finally, the battery cell chemistries are compared in the outlook for vehicle implementation. Section 4 comprehensively discusses the findings, while Section 5 summarizes the main conclusions and implications.

## 2. Method

The use-case analysis follows the methodology illustrated in Fig. 1. A complete factorial analysis initially incorporates two primary variables: the electric vehicle's implemented battery capacity and a representative distance defined as a trip range. Battery capacity and trip range represent critical vehicle engineering factors that significantly influence the application potential of SIB in BEVs. These parameters are inputs for the longitudinal dynamics simulation (LDS) performed for three distinct battery cell chemistries: NMC, LFP, and SIB. Within the LDS, a electric reference vehicle is simulated, allowing for systematic determination of how different battery cell chemistries affect vehicle performance parameters. The LDS is parameterized using battery cell characteristics from an extensive literature review, with the energy consumption results validated against empirical data. The simulation outputs are fed into a cost model, incorporating relevant economic parameters, including specific cell and operational costs. This cost model enables quantitative assessment of the economic implications of implementing SIB technology in electric vehicles. Based on the simulation results and subsequent cost modeling, a systematic comparison of the three battery cell chemistries is performed at the vehicle level, evaluating key metrics such as battery-related cost or the maximum vehicle range depending on the battery chemistry. The methodology employed is based initially on the work of Teichert et al. [28] and Schneider et al. [29] but has been adapted specifically for BEV applications and modified to accommodate the intended analytical approach for use-case analysis of SIBs in BEVs.

### 2.1. Vehicle simulation

A LDS approach based on the work of König et al. [33] was implemented to conduct the vehicle-level analysis of SIB technology. The Volkswagen (VW) ID.3 is used as the reference vehicle for this analysis. Its status as a mass-produced, purely electric vehicle in the compact segment justifies this selection, making it representative for the analytical framework [34]. The specific model variant utilized in this analysis is the VW ID.3 Pro Performance from 2020. A characteristic of this BEV is its availability with multiple battery storage systems offering net energy contents of 45 kWh, 58 kWh, and 77 kWh [35]. This variable battery configuration within the same vehicle platform provides a foundation for analyzing the effects of varying battery capacities on achievable driving ranges and the implications of battery-related costs. Furthermore, the analysis accounts for packaging constraints imposed by the reference vehicle's battery pack dimensions, establishing upper limits for the installable battery capacity. The reference vehicle VW ID.3 employs NMC battery cell chemistry across all configurations [35]. The vehicle simulation framework extends beyond this standard NMC case, including theoretical configurations with LFP

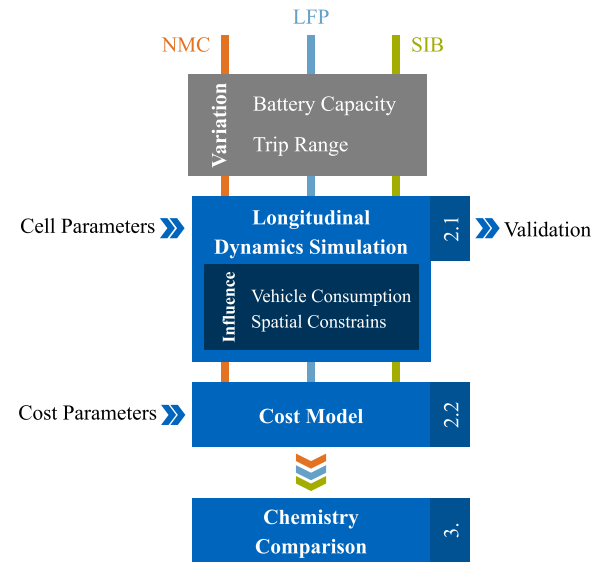


Fig. 1. Schematic overview of the method applied for the use-case analysis of SIB technology in BEVs.

and SIB cell chemistries. The LFP battery chemistry positions itself between NMC and SIB technologies considering gravimetric and volumetric energy density [29,32]. This intermediate position enables LFP to function as a transitional reference point in the analysis. Including LFP also provides valuable insights for technology assessment and cell selection, facilitating the identification of optimal use-cases for each chemistry. NCA battery chemistry is excluded from this analysis, as its energy density characteristics and specific costs closely parallel those of NMC cells [32]. The key differentiating parameters between SIBs and the analyzed LIB cells are gravimetric and volumetric energy densities and specific battery costs [32].

The LDS provides critical outputs by simulating the effects of varying battery cell chemistry and implemented battery capacity. For each vehicle configuration, the simulation calculates energy consumption in kWh/100 km, which directly determines the achievable maximum range of the vehicle. A key modeling assumption in this approach is that battery weight, which varies based on the chosen cell chemistry and implemented battery capacity, directly influences the simulated energy efficiency and overall vehicle performance. Additionally, the simulation accounts for spatial constraints within the reference vehicle, providing information about the maximum implementable battery capacity for each chemistry based on volumetric limitations.

Calculating vehicle configurations with varying battery capacities and cell chemistries is conducted according to the following steps. The vehicle mass calculations are performed using Eqs. (1) and (2). The gross vehicle weight  $m_{g,vw}$  is determined by combining the vehicle mass without battery and the battery mass  $m_{bat}$ . The vehicle mass without battery  $m_{wo,bat}$  is fixed at 1462 kg [33]. The battery mass is calculated for each increment of battery capacity  $E_{bat}$ , incorporating cell-specific parameters, including gravimetric energy density  $\rho_{grav}$  and the gravimetric cell-to-pack factor  $z_{c2p,grav}$ .

$$m_{g,vw} = m_{wo,bat} + m_{bat} \quad (1)$$

$$m_{bat} = \frac{E_{bat}}{\rho_{grav} z_{c2p,grav}} \quad (2)$$

The volumetric calculation of the battery pack is expressed in Eq. (3). This calculation follows a similar approach to Eq. (2) but employs the volumetric energy density  $\rho_{vol}$  and the volumetric cell-to-pack

factor  $z_{c2p,vol}$ . The maximum available packaging space  $V_{bat,max}$ , which constitutes the upper limit for battery implementation, is 289 L [35].

$$V_{bat} = \frac{E_{bat}}{\rho_{vol} z_{c2p,vol}} \quad (3)$$

The vehicle simulation was pointwise validated using empirical data from Wassiliadis et al. [35]. Their study analyzed the VW ID.3 Pro Performance from 2020 with a 58 kWh battery capacity. The LDS demonstrated high accuracy, with deviations in energy consumption for the 58 kWh NMC configuration between simulated and experimentally determined values being less than 10% for the Worldwide harmonized Light vehicles Test Procedure (WLTP) cycle. Additional validation was performed using the Federal Test Procedure 75 (FTP75) driving cycle, where differences between simulated and experimental energy consumption were less than 5%.

## 2.2. Cost model

The cost model focuses solely on battery-related costs when comparing different battery configurations. This targeted approach is justified since the battery pack represents the only differentiating component within the analysis scope, while all other vehicle components remain identical. The battery-related costs  $C_{BatRelated}$  comprise the battery investment costs  $C_{bat,inv}$ , energy costs  $C_{bat,energy}$ , and resale profit  $C_{bat,res}$ , which is subtracted from the total costs, as shown in Eq. (4).

$$C_{BatRelated} = C_{bat,inv} + C_{bat,energy} - C_{bat,res} \quad (4)$$

The battery investment costs are determined by the battery-related cost parameters and the implemented battery capacity  $E_{bat}$ , as shown in Eq. (5). The battery-related cost parameters include the specific battery costs  $c_{spec}$ , which differ depending on the battery cell chemistry, and a scaling factor from cell to system level  $z_{c,c2p}$ .

$$C_{bat,inv} = c_{spec} z_{c,c2p} E_{bat} \quad (5)$$

The energy costs required for operating the electric vehicle are calculated based on normalized energy costs per kilometer  $C_{bat,ene}$ , and the total vehicle mileage  $S_{tot}$ , according to Eq. (6). Based on the work of Schloter [36], a total mileage of 160.000 km was defined, representing a typical ownership period until vehicle resale. This assumed mileage aligns with established values for passenger vehicle ownership cycles, corresponding to approximately ten years of vehicle operation [36–38].

$$C_{bat,energy} = C_{bat,ene} S_{tot} \quad (6)$$

The normalized energy costs per kilometer are determined by the energy consumption in kWh per kilometer  $f_{cons}$ . This value varies with the implemented battery capacity in the electric vehicle, as it directly correlates with the battery weight, as shown in Eq. (2). The normalized energy cost per kilometer also depends on the specific energy cost  $c_{ene}$ , a function of the trip distance  $S_{trip}$ . The complete relationship between these parameters is expressed in Eq. (7).

$$C_{bat,ene} = f_{cons}(E_{bat}) c_{ene}(S_{trip}) \quad (7)$$

The specific energy cost  $c_{ene}$  varies with the trip distance  $S_{trip}$ .  $S_{max,r}$  represents the maximum range achievable with a fully charged battery without recharging. This value is derived from vehicle simulation and directly depends on the implemented battery capacity in the electric vehicle. The specific energy cost corresponds to the home charging price  $c_{hoc}$  for trip distances less than or equal to the maximum range. This relationship is formally expressed in Eq. (8). For trip distances exceeding the maximum range, external charging becomes necessary. This charging occurs at a higher electricity price, denoted as external charge cost  $c_{extc}$ . The proportion of kilometers driven using home charging versus external charging is calculated based on the trip distance, as shown in Eq. (9). This calculation utilizes the share of home-

**Table 2**  
Cell and cost parameters used in the vehicle simulation and cost model.

Section	Symbol	Value	Source
Vehicle simulation	$m_{wo,bat}$	1462 kg	[35]
	$V_{bat,max}$	289 L	[35]
	$\rho_{grav,NMC}$	273 Wh kg <sup>-1</sup>	[29]
	$\rho_{grav,LFP}$	176 Wh kg <sup>-1</sup>	[29]
	$\rho_{grav,SIB}$	140 Wh kg <sup>-1</sup>	[32]
	$z_{c2p,grav,NMC}$	0.59	[29]
	$z_{c2p,grav,LFP}$	0.71	[29]
	$z_{c2p,grav,SIB}$	0.71	<sup>a</sup>
	$\rho_{vol,NMC}$	685 Wh L <sup>-1</sup>	[29]
	$\rho_{vol,LFP}$	450 Wh L <sup>-1</sup>	[32]
	$\rho_{vol,SIB}$	375 Wh L <sup>-1</sup>	[32]
	$z_{c2p,vol,NMC}$	0.39	[29]
	$z_{c2p,vol,LFP}$	0.55	[29]
$z_{c2p,vol,SIB}$	0.55	<sup>a</sup>	
Cost model	$S_{tot}$	160.000 km	[36]
	$r_{res}$	30%	[36]
	$c_{spec,NMC}$	100 € kWh <sup>-1</sup>	[32]
	$c_{spec,LFP}$	80 € kWh <sup>-1</sup>	[32]
	$c_{spec,SIB}$	50 € kWh <sup>-1</sup>	[32]
	$z_{c,c2s}$	2.07	[29]
	$c_{hoc}$	0.37 € kWh <sup>-1</sup>	[41]
$c_{extc}$	0.70 € kWh <sup>-1</sup>	[42]	

<sup>a</sup> Based on Mei et al. [39], Kim [40] and Rudola et al. [22], SIBs have similar thermal stability properties to LFP cells. So, the same cell-to-pack factors of LFP and SIBs are chosen.

charged energy  $z_{hoc}$ , determined by the ratio of maximum range to trip distance, as expressed in Eq. (10).

$$S_{trip} \leq S_{max,r} : c_{ene} = c_{hoc} \quad (8)$$

$$S_{trip} > S_{max,r} : c_{ene} = z_{hoc} c_{hoc} + (1 - z_{hoc}) c_{extc} \quad (9)$$

$$z_{hoc} = \frac{S_{max,r}}{S_{trip}} \quad (10)$$

The resale profit  $C_{bat,res}$  represents the residual value of the initial battery pack. Following Schloter [36], for a vehicle ownership period of ten years and corresponding mileage of 160.000 km, the resale value  $r_{res}$  corresponds to 30% of the initial investment cost of the vehicle, as shown in Eq. (11). Since the entire electric vehicle is resold after this period of use, the same depreciation rate is applied to the battery component.

$$C_{bat,res} = r_{res} C_{bat,inv} \quad (11)$$

To evaluate the battery-related trip costs per kilometer  $C_{Bat,Trip}$  within the analysis framework, the battery-related costs are divided by the total mileage. This normalization enables a comparative assessment of distance-specific battery costs across the entire investigation scope, as expressed in Eq. (12).

$$C_{Bat,Trip} = \frac{C_{BatRelated}}{S_{tot}} \quad (12)$$

The system parameters employed in the vehicle simulation and cost model are presented in Table 2. The parameters for SIBs are primarily based on the work of Hasselwander et al. [32], as this publication provides a detailed characterization of potential future cell chemistries, including SIBs. Due to the absence of commercially available vehicles with SIBs, gravimetric and volumetric cell-to-pack factors could only be estimated theoretically. These estimations draw upon research by Mei et al. [39], Kim [40] and Rudola et al. [22], which demonstrate that SIBs exhibit thermal stability characteristics comparable to LFP cells. Based on these similarities, it can be anticipated that SIBs would utilize battery pack designs with cell-to-pack ratios similar to LFP systems. Consequently, for this analytical framework, the cell-to-pack factors for SIBs were assumed to be equivalent to those of LFP cells.

### 3. Results

Based on the methodology described above, the following section presents the results addressing the two proposed research questions. Section 3.1 individually examines the cost-effectiveness of the three battery cell chemistries, NMC, LFP, and SIB, based on battery capacity and trip range. Building on these findings, Section 3.2 analyzes the interrelationships between these cell chemistries and shows their comparative advantages and trade-offs. Section 3.3 investigates how energy cost parameters influence the overall cost analysis. Section 3.4 quantifies the sensitivities of SIB cell characteristics to the vehicle-relevant cost properties. Finally, Section 3.5 describes the challenges and potentials of implementing SIB technology in electric vehicles through limit value configurations.

#### 3.1. Cost-efficiency analysis depending on the battery capacity and trip range

This section addresses the question of which cell chemistry is most cost-effective in terms of trip range and implemented battery capacity. Fig. 2 presents the analysis for the reference vehicle equipped with an NMC battery. The x-axis represents the range of theoretically implemented battery capacities in the reference vehicle. The y-axis displays trip ranges from 0 km to 600 km, representing round trips that begin and end at a home charging source. The legend represents the battery-related trip costs in € per 100 km. So, the battery-related costs for trip ranges are shown depending on the battery capacity implemented in the reference vehicle.

As evident in Fig. 2, the maximum range, depicted by a white line, increases proportionally with the battery capacity implemented in the electric vehicle. This line divides the figure into two regions: the area below represents trips without recharging, while in the area above, recharging becomes necessary to achieve desired trip distances. The region below the maximum range line demonstrates a linear increase in battery-related trip costs with increasing battery capacity. This correlation can be attributed to two factors that increase with battery capacity in the reference vehicle: consumption due to increased battery weight and investment costs due to the requirement for additional battery cells. This relationship becomes apparent as an increase in battery-related trip costs per kilometer. Beyond the maximum range line, the proportion of external charging required to achieve the trip range must be considered. As shown in Table 2, the external charge has higher costs, resulting in an observable cost increase per kilometer for each battery capacity as the trip range increases. This creates a trade-off between accepting higher recharging costs or increasing battery capacity to extend the maximum range. The highest battery-related costs per kilometer occur in the upper-right area with high battery capacities at extended trip ranges. The most cost-efficient configurations are found at lower battery capacities and trip ranges up to the maximum range line.

The contour lines in Fig. 2 exhibit a downward trend in the upper area where recharging occurs, indicating increasing trip costs with higher battery capacities. This trend emerges because investment costs exceed external charging costs for NMC batteries. So, it proves more cost-efficient to rely on external charging rather than implementing a larger battery capacity. This cost behavior can be attributed to NMC being the most expensive battery cell chemistry with high specific battery costs, which exerts a more significant influence on battery-related trip costs per kilometer than recharging costs.

Fig. 3 presents the analysis with the reference vehicle's theoretically implemented LFP battery cell chemistry. The maximum range of the LFP configuration is slightly lower than in the NMC battery analysis. Additionally, the general cost level of this analysis is lower than for NMC batteries, as evident in the legend of Fig. 3. The general relationships, however, remain comparable. Notable are the spatial constraints beginning at 71 kWh, represented by a hatched box. These packaging

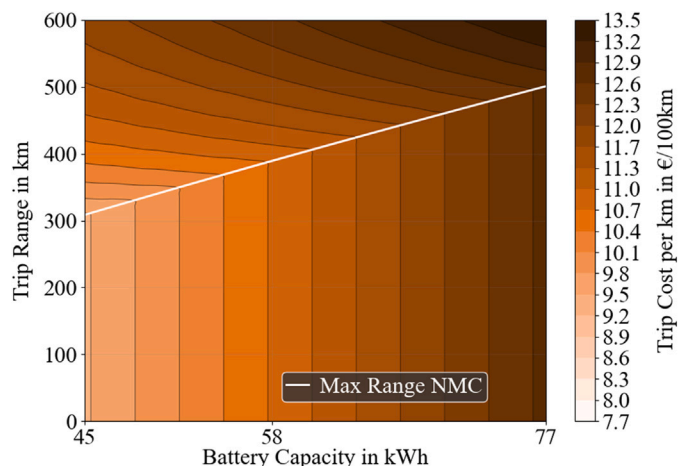


Fig. 2. Use-Case NMC Battery: Battery-related costs per 100 km by battery capacity and trip range. Trip costs range from 13.5 €/100 km to 9.5 €/100 km.

limitations can be attributed to the lower volumetric energy density of LFP battery cells. In the upper area, where recharging is necessary, a downward trend in the contour lines is also observable, particularly in trip ranges exceeding 450 km. However, this downward trend is less pronounced than in the NMC battery case. Notably, in the upper area between 300 km and 400 km, an almost horizontal progression of the contour lines can be observed. This indicates an equilibrium between recharging and investment costs. It has equivalent cost implications per kilometer, whether implementing a smaller battery with a more significant proportion of external charging or a larger battery with minimal or no recharging due to increased maximum range. This trend can be attributed to the lower specific battery costs of LFP compared to NMC batteries.

Fig. 4 presents the analysis of the reference vehicle with theoretically implemented SIBs. The maximum range in dependence on the battery capacity is lower than in the studies with NMC and LFP batteries. Additionally, the cost level of trip costs per kilometer, as shown in the legend of Fig. 4, is also lower than in both previously examined battery configurations.

In contrast to the previously presented battery chemistries, the SIB configuration exhibits more pronounced spatial constraints due to its lower volumetric energy density. This lower volumetric energy density constrains feasible configurations of the reference vehicle to battery capacities between 45 kWh to 59 kWh, significantly limiting the solution space to small and medium battery capacities. The contour lines in the upper area with recharging show a slight downward trend transitioning to horizontal progression with decreasing trip ranges between 450 km and 650 km. The region with trip ranges below 450 km is particularly interesting, where a slight upward trend in the contour lines becomes apparent. According to the cost model, recharging costs dominate over investment costs in this region. Therefore, in this range, it becomes economically advantageous to implement more battery capacity in the reference vehicle to avoid recharging, which is associated with higher costs. This behavior can be attributed to SIB's significantly lower battery-specific costs than LFP and particularly NMC, resulting in lower investment costs. At the same time, recharging maintains a dominant influence on overall costs, leading to a slight upward trend of the contour lines in this area.

#### 3.2. Comparative cost representation depending on the battery capacity

The following analysis compares the previously presented chemistry-specific results to evaluate their comparative impacts on vehicle-related properties. Fig. 5 presents this comparison through the

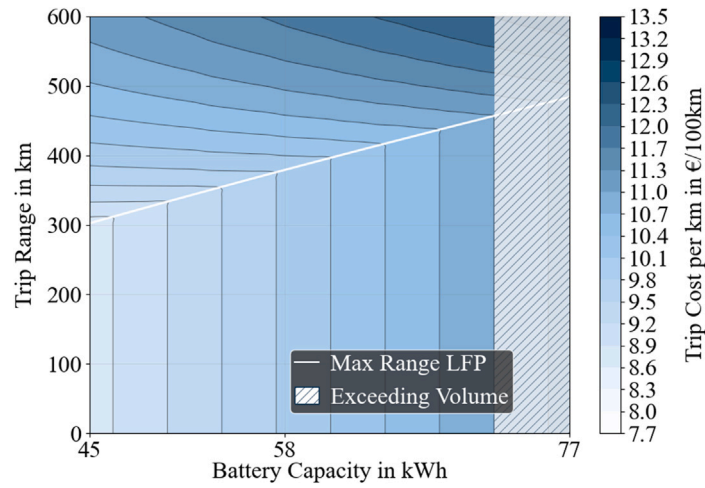


Fig. 3. Use-Case LFP Battery: Battery-related costs per 100 km by battery capacity and trip range. Hatched regions depict areas where spatial restrictions of the battery are exceeded. Trip costs in the viable area range from 12.3 €/100 km to 8.8 €/100 km.

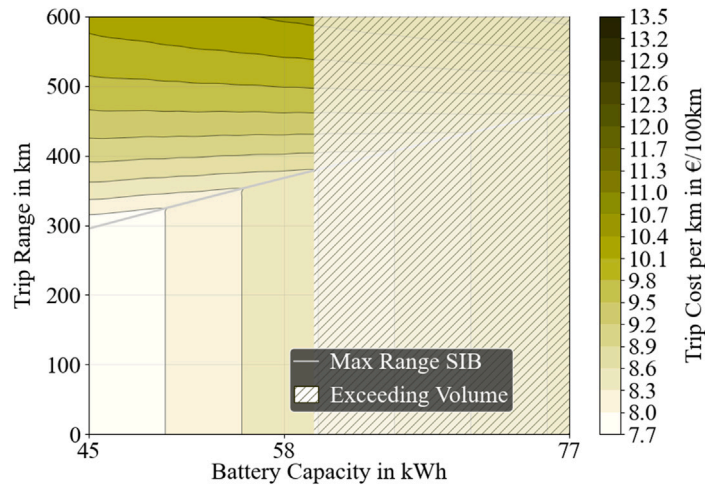


Fig. 4. Use-Case SIB Battery: Battery-related costs per 100 km by battery capacity and trip range. Hatched regions depict areas where spatial restrictions of the battery are exceeded. Trip costs in the viable area range from 10.5 €/100 km to 7.7 €/100 km.

three sub-figures (a), (b), and (c), showing the battery-related costs per 100 km for NMC, LFP, and SIB cell chemistries at three different battery capacities of the reference vehicle. The battery capacities examined are 45 kWh, 58 kWh, and 77 kWh, representing minimum, medium, and maximum configurations, respectively, encompassing the complete analysis spectrum.

The difference in the achievable maximum range between the NMC and SIB vehicle configuration in Fig. 5(a) is approximately 15 km. This slight difference can be attributed to the relatively small battery capacity at 45 kWh and the consequent implications on the battery weight. The additional weight and consequently increased consumption due to SIB cell chemistry’s lower gravimetric energy density has less impact, given the reference vehicle’s high base weight without the battery pack. In Fig. 5(b) the maximum range levels for all battery chemistries increase. The difference between SIB and NMC configurations considering maximum range amounts to 22 km. This increased difference can be attributed to the higher implemented battery capacity, which amplifies the effects of gravimetric energy density differences and associated consumption variations. For the 77 kWh battery capacity in Fig. 5(c) the difference in maximum range between SIB and NMC amounts to 34 km.

In Fig. 5(a) the reference vehicle with a SIB battery demonstrates 19.3% lower battery-related costs per kilometer than the NMC configuration. In Fig. 5(b) the general cost level for all three battery

chemistries has increased compared to the minimum configuration. In this case, the cost savings from NMC to SIB regarding cost per kilometer amounts to 21.8%. This more significant cost difference can be attributed to the correlation between SIB’s lower investment costs and increased battery capacity. For the LFP configurations, the battery-related costs and the maximum ranges fall between SIB and NMC levels but remain closer to NMC in terms of cost level. For Fig. 5(c) the cost per kilometer reduction from NMC to SIB reaches its highest value with 24.2%. However, the LFP and SIB configurations exceed the maximum battery package volume due to their lower volumetric energy densities. Therefore, these findings remain hypothetical, as these configurations do not represent viable configurations according to the use-case analysis methodology. In the regions requiring recharging, similar cost-per-kilometer proportions like for trip ranges below the maximum range persist, though the cost differences become slightly smaller. This reduction in cost difference occurs because SIB and LFP configurations must utilize more expensive recharging earlier in the driven trip range compared to the NMC configuration.

SIBs would achieve cost parity with LFP batteries in terms of costs per kilometer at a specific battery cost of 76.5 €/kWh<sup>-1</sup>. This cost parity point was determined through an iterative analysis where all parameters were held constant while only varying the battery-specific costs of the SIB until cost equivalence was reached. This lower cell price is required due to SIB’s inferior gravimetric energy density, necessitating

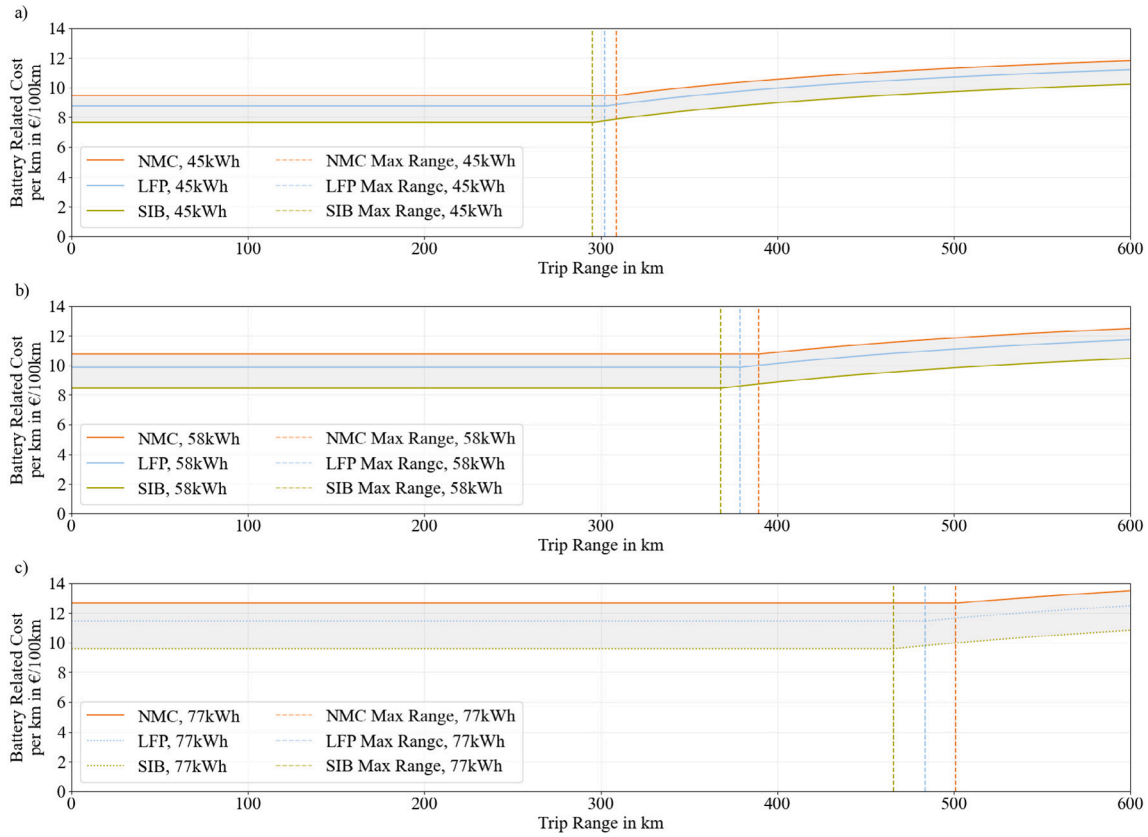


Fig. 5. Battery-related costs per kilometer for NMC, LFP and SIB cell chemistries at various battery capacities. Fig. 5(a) represents the minimum battery capacity at 45kWh, Fig. 5(b) shows the medium battery capacity at 58kWh and Fig. 5(c) depicts the maximum battery capacity at 77kWh.

compensation for increased energy consumption. Consequently, SIB advantages are only present with a significant cell price differential compared to LFP technology. The use-case analysis shows that SIB must be at least  $3.5 \text{ € kWh}^{-1}$  cheaper in cell price than LFP to be competitive. Otherwise, LFP battery technology demonstrates advantages through superior range and reduced packaging space requirements due to better gravimetric and volumetric energy density. However, the battery-specific costs of SIBs, as assumed in Table 2, are significantly lower than LFP.

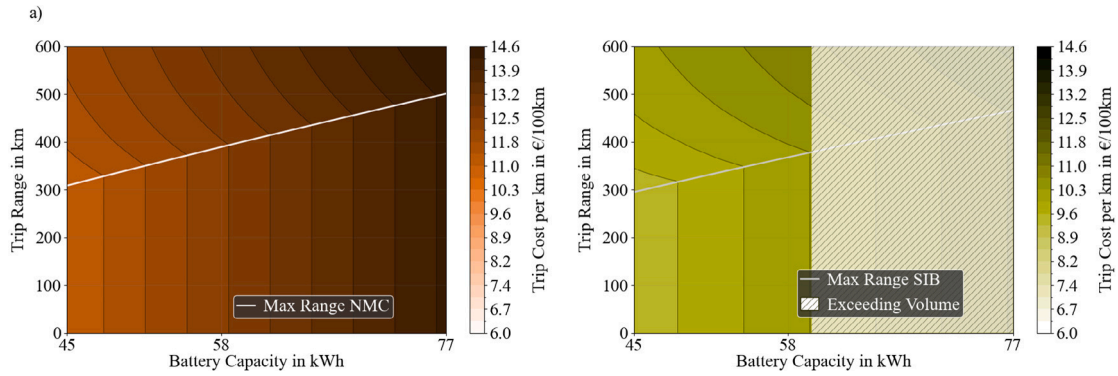
### 3.3. Influence of cost differences in charging prices on trip costs

The following section examines how differences in energy prices, specifically home and external charging, affect the analysis results. The analysis focuses on NMC and SIB configurations. In the previous two sections, the study utilized the home and external charging costs depicted in Table 2. These values establish a delta between home and external charging costs of  $0.33 \text{ € kWh}^{-1}$ . For the NMC case, this price structure resulted in a tendency toward lower battery capacities regarding trip costs per kilometer, as investment costs dominate the battery-related costs. In the SIB case, recharging costs dominated the cost model below 450 km, making increased battery capacity advantageous from a cost perspective. To systematically analyze the impact of varying price differences, the reference delta is varied by  $\pm 0.22 \text{ € kWh}^{-1}$ , resulting in representative extreme cases of  $0.11 \text{ € kWh}^{-1}$  and  $0.55 \text{ € kWh}^{-1}$ , respectively.

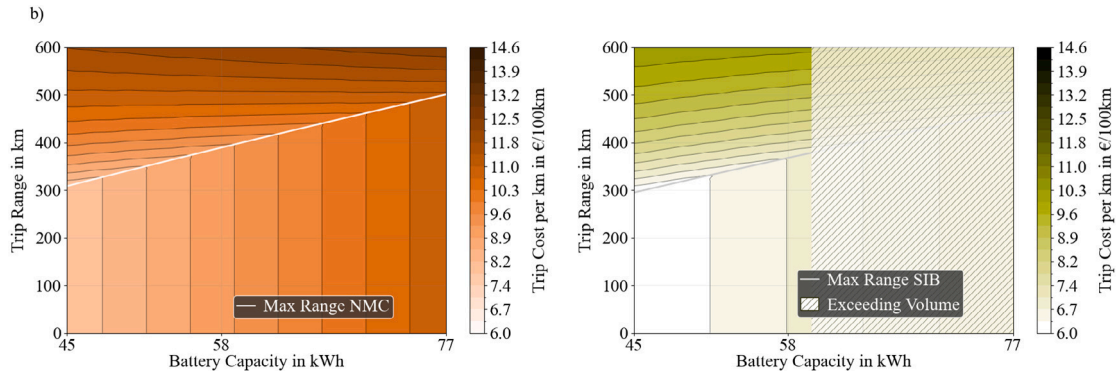
To evaluate the plausible extreme case of high home and lower external charging costs, Fig. 6(a) presents the results calculated with home charging cost  $c_{\text{hoc}}$  of  $0.48 \text{ € kWh}^{-1}$  and external charging cost  $c_{\text{extc}}$  of  $0.59 \text{ € kWh}^{-1}$ . This reduces the cost delta to  $0.11 \text{ € kWh}^{-1}$ . Fig. 6(a) demonstrates that both cell chemistries exhibit a steep downward

trend in the contour lines with increasing battery capacity in the trip range region requiring recharging. This downward trend appears more pronounced for the NMC compared to the SIB scenario. This behavior can be attributed to investment costs dominating the cost model in this scenario, as the difference between home and external charging becomes less significant. Consequently, the tendency for lower trip costs per kilometer shifts toward configurations with lower battery capacities, with high battery capacity becoming more a comfort factor than a cost-saving measure.

Fig. 6(b) shows the impact of low home and high external charging costs on the use-case analysis. In this scenario, home charging costs  $c_{\text{hoc}}$  equal  $0.26 \text{ € kWh}^{-1}$ , and external charging costs  $c_{\text{extc}}$  correspond to  $0.81 \text{ € kWh}^{-1}$ , representing another possible extreme case. The delta between these charging cost prices amounts to  $0.55 \text{ € kWh}^{-1}$ . Both analyzed battery cell chemistries exhibit an upward trend in contour lines in regions requiring recharging. This increase appears less pronounced for NMC, resulting in horizontal to slightly declining contour line progression in high trip ranges above approximately 500 km. The significant rise in contour lines in the recharging region for SIB indicates that high recharging costs strongly influence the analysis results in this case. Recharging is thus associated with high additional costs, making it advantageous to implement a larger battery capacity in the reference vehicle for lower trip costs per kilometer, thereby utilizing the increase in maximum range. The case of low installed battery capacity combined with high trip ranges results in the highest trip costs per kilometer, as large proportions of expensive external charging relative to cheap home charging are required for propulsion. These relationships also exist for NMC up to trip ranges of 450 km, though less pronounced due to higher battery investment costs, which limit the cost advantages of increasing battery capacity.



(a) Fig. 6(a): Battery-related trip cost with a small  $0.11 \text{ € kWh}^{-1}$  delta between home and external charging costs. Trip costs for NMC range from  $14.6 \text{ €/100 km}$  to  $11.1 \text{ €/100 km}$ . For SIB, trip costs in the viable area range from  $11.0 \text{ €/100 km}$  to  $9.4 \text{ €/100 km}$ .



(b) Fig. 6(b): Battery-related trip cost with a significant delta of  $0.55 \text{ € kWh}^{-1}$  between home and external charging costs. Trip costs for NMC range from  $12.3 \text{ €/100 km}$  to  $7.9 \text{ €/100 km}$ . For SIB, trip costs in the viable area range from  $10.0 \text{ €/100 km}$  to  $6.0 \text{ €/100 km}$ .

Fig. 6. Influences of changes in home and external charging costs on the battery-related trip costs. Hatched regions depict areas where spatial restrictions of the battery are exceeded.

### 3.4. Vehicle-related effects of changes in the cell properties of sodium-ion cells

The following section analyzes and quantifies the vehicle-related impacts of varying SIB cell characteristics through a sensitivity analysis presented in Fig. 7. The sensitivity analysis evaluates how changes in cell characteristics impact overall vehicle performance and costs, thereby quantifying the uncertainties associated with implementing SIB cells in electric vehicle applications. The x-axis shows the theoretical battery capacity of the reference vehicle, while the y-axis displays the battery-related trip costs per kilometer. The sensitivity analysis considers only scenarios where vehicle propulsion relies on home charging, excluding recharging. The central SIB line illustrates how battery-related costs per kilometer for the SIB configuration evolve across different implemented battery capacities in the reference vehicle. Additionally, non-feasible SIB configurations are indicated by dotted lines, as configurations above  $59 \text{ kWh}$  exceed spatial constraints due to the lower volumetric energy density.

The gravimetric energy density of the SIB cell is varied by  $\pm 10\%$  from the baseline value shown in Table 2. The analysis reveals that SIB cell gravimetric energy density variations lead to a relatively minor change in battery-related costs per kilometer of  $\pm 1\%$ . This limited sensitivity can be attributed to changes in energy consumption due to vehicle mass variations, whether increases or decreases, having a comparatively small impact on overall costs per kilometer. This effect is particularly pronounced given the high total mass of the reference vehicle, where battery mass variations represent only marginal changes relative to the overall vehicle mass.

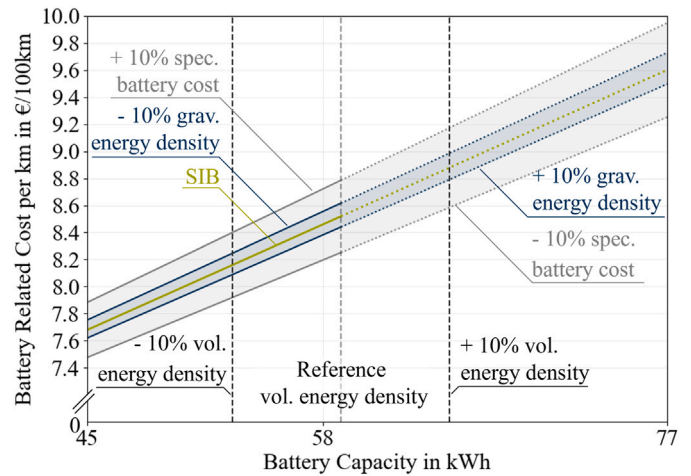


Fig. 7. Sensitivity analysis of battery cell characteristics of SIB cell on the battery-related costs per kilometer. The battery cell characteristics comprise of SIB's gravimetric energy density, specific battery costs, and the volumetric energy density.

The specific battery costs of the SIB cell from Table 2 were varied by  $\pm 10\%$ . As shown in Fig. 7, the sensitivity to specific SIB costs demonstrates a more substantial influence in battery-related costs per kilometer of  $\pm 3.2\%$ . This stronger correlation can be attributed to the

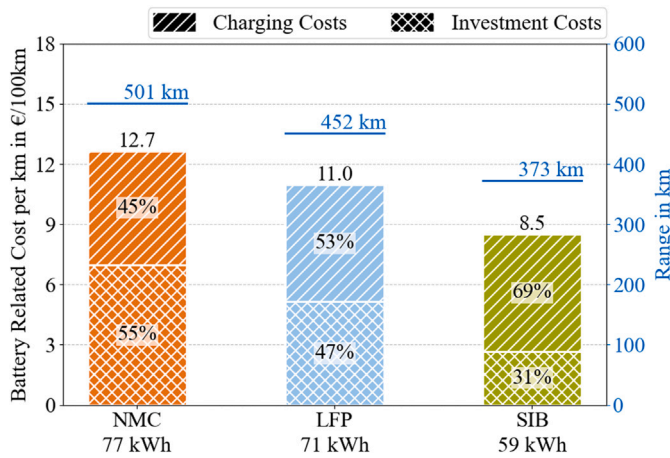


Fig. 8. Comparison of battery-related costs per km and maximum range for the highest feasible battery capacity configurations of each cell chemistry.

direct influence of specific battery costs on battery investment costs, directly affecting costs per kilometer. Consequently, the magnitude of this effect is more pronounced.

The spatial constraints of the battery pack occur at battery capacities exceeding 59 kWh. This limitation is visualized in Fig. 7 through a vertical line and dotted continuations of the cost per kilometer curves. The volumetric energy density of SIB cells is also subjected to sensitivity analysis, varying by  $\pm 10\%$  from the baseline value assumed in Table 2. A 10% reduction in volumetric energy density results in spatial constraints for the reference vehicle at battery capacities exceeding 53 kWh, significantly restricting the solution space and severely limiting feasible configurations. Conversely, a 10% increase in SIB cell volumetric energy density enables configurations with battery capacities up to 65 kWh, substantially expanding the range of viable vehicle configurations within the investigation framework.

### 3.5. Comparative battery assessment for vehicle implementation using limit value considerations

This section presents limit value considerations of implemented battery capacities to evaluate the application, limitations, and opportunities of the three considered battery chemistries in electric vehicles. The analysis is structured in two comparative scenarios to establish the technical boundaries. In the first case, maximum battery capacity configurations in the reference vehicle are evaluated for each battery chemistry, defining the upper technical limits. In the second case, minimum LIB capacity configurations are compared against maximum SIB configurations.

Fig. 8 compares the characteristics of reference vehicles equipped with the maximum battery capacity configuration achievable for each chemistry. Due to differences in volumetric energy density, the maximum feasible battery configurations under spatial battery pack restrictions are 77 kWh for NMC, 71 kWh for LFP, and 59 kWh for SIB. The costs reflect home-charging for vehicle propulsion for better comparability.

The analysis reveals that NMC exhibits the highest costs, followed by LFP, while SIB shows the lowest trip costs. The cost advantages of LFP and SIB are due to lower battery investment costs and lower implemented battery capacities in the respective reference vehicles. The cost structure breakdown shows that for NMC, 55% of the costs per kilometer are attributed to investment costs. In the case of LFP, investment costs represent 47% of the cost per kilometer. With 31%, the SIB configuration demonstrates significantly lower investment costs than the other battery chemistries, reducing costs per kilometer. The

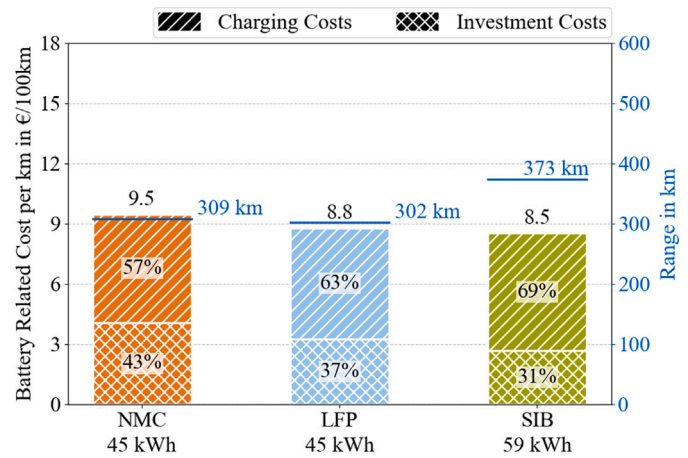


Fig. 9. Comparison of battery-related costs per km and maximum range for minimum LIB capacity configurations and maximum SIB capacity configuration.

analysis indicates that charging costs for vehicle propulsion remain comparable across the battery chemistries due to counterbalancing effects. The NMC configuration shows increased vehicle mass due to higher battery capacity. In contrast, the SIB configuration exhibits similar consumption values despite lower battery capacity due to inferior gravimetric energy density. The LFP configuration presents intermediate characteristics between these extremes. These opposing factors result in negligible differences in charging costs across the battery configurations.

Analysis of maximum achievable ranges reveals distinct performance characteristics between the battery chemistries, with NMC enabling the highest driving distances without recharging. LFP and SIB configurations achieve maximum ranges of 49 km and 128 km lower than NMC within the defined investigation framework. These findings highlight the current limitations of SIB chemistry regarding range capabilities and emphasize the necessity for recharging in SIB configurations.

Fig. 9 illustrates the differences in cost per kilometer and maximum range between minimal LIB battery capacity and maximum SIB configurations. The comparison considers a 45 kWh battery capacity for NMC and LFP, and 59 kWh for the SIB configuration. The results reveal that NMC has higher costs per kilometer despite its lower battery capacity than SIB. LFP also shows increased costs compared to SIB. These cost relationships can be attributed to SIB's lower investment costs due to reduced specific battery costs despite its higher capacity. The charging costs remain comparable across battery chemistries, consistent with the findings in Fig. 8. SIB technology's lower specific battery costs emerge as a decisive factor in determining the overall cost per kilometer, significantly influencing the investment costs.

Investigation of the maximum range across the battery chemistries shows that the SIB configuration achieves the highest maximum range of 373 km due to its comparatively high implemented battery capacity in the reference vehicle. In contrast, NMC and LFP configurations demonstrate lower maximum ranges of 309 km and 302 km, respectively. This relationship is particularly significant as it indicates that SIB configurations can achieve higher maximum range and lower costs per kilometer, representing a notable advantage over LIB configurations.

## 4. Discussion

This study comprehensively analyzes the impacts of the SIB technology on vehicle-related cost and performance parameters. Our analysis extends the existing literature by offering a structured approach to evaluating battery technology innovations in electric vehicles while

providing novel insights into the automotive implementation of SIB technology.

According to Xu et al. [43], electric vehicles can be categorized into three segments based on battery capacity: small, mid-size, and large. The battery capacities of 45 kWh, 58 kWh, and 77 kWh analyzed in this study represent these segments, respectively. The analysis reveals that SIB vehicles face significant spatial constraints, limiting their feasibility primarily to small and mid-size vehicle segments within the investigation framework. However, these limitations align well with one of the promising application areas for SIB technology: the commuter vehicle segment. According to multiple studies, daily commuting distances typically range from 34 km to 100 km for round trips [22,44,45]. These distances correspond to the requirements of the small vehicle segment. According to the results of this study, SIB technology has the lowest cost per kilometer of all the battery chemistries examined in this segment. With ranges of up to 298 km for the 45 kWh configuration, SIB even exceeds the range requirements for the commuter segment. The mid-size segment is another compelling application area for SIB technology. Results show that SIBs are also establishing themselves as the most cost-efficient battery cell chemistry in this segment. The mid-size segment is considered the all-rounder segment, which the SIB configuration addresses with a range of up to 373 km using a 59 kWh configuration. The findings indicate that implementing maximum battery capacity in the SIB configuration proves economically advantageous. This is because the additional investment costs from the larger battery have less impact on total costs than external recharging across a wide range of trip distances. This economic advantage is particularly pronounced when low-cost home charging options are available, such as those enabled by photovoltaic systems. At higher charging prices, the cost advantages of SIBs are not as pronounced; however, as shown in Fig. 6, they remain economically more efficient compared to the NMC configuration. Additionally, implementing the maximum battery capacity would offer both cost advantages and environmental benefits, as SIBs are considered more sustainable and environmentally friendly than LIBs [46,47]. Fig. 9 illustrates that electric vehicles with SIB in the mid-size segment are more cost-efficient than LIB configurations in the small segment while providing an additional 60 km range. The large electric vehicle segment, representing the luxury and comfort segment typically featuring high battery capacities for extended ranges, proves unsuitable for SIB configurations. Despite the higher costs, NMC battery technology is particularly fitting for this vehicle segment with its high gravimetric and volumetric energy density, as customers in this premium market segment are willing to accept the additional expenses. LFP battery chemistry represents a balanced solution, offering economic advantages between SIB and NMC battery chemistries. With LFP technology positioning itself closer to NMC's capabilities, it shows potential to enter the large vehicle segment with future improvements in energy density.

The analysis developed for this study exhibits certain limitations and simplifications. It must be noted that SIB cells are still in the research stage and not fully commercialized. While we attempted to select the most suitable and reliable analysis parameters for SIBs, these values remain theoretical and must be considered as such. We conducted a comprehensive sensitivity analysis on these parameters to address this uncertainty and ensure transparency. Beyond data-related limitations, several methodological constraints should be noted. The choice of the reference vehicle influences the results regarding battery packaging space and powertrain efficiency. Battery aging effects are incorporated through resale value calculations for model simplification. The analysis employs basic vehicle operation assumptions, assuming trips begin with a fully charged battery and charging infrastructure availability. Additionally, using the WLTP cycle may not fully represent real-world driving conditions, as individual driving profiles can vary. Nevertheless, this work establishes an analytical framework applicable to the early development stages of electric vehicles, with underlying data available upon request.

## 5. Conclusion

The innovation analysis of novel battery cells for electric vehicles represents a crucial factor in advancing electromobility. This paper presents an analytical framework for evaluating the potential of SIBs in electric vehicles by examining vehicle-related and cost-related implications of selecting SIBs compared to NMC and LFP cells. Results demonstrate the cost advantages of SIBs over both alternative cell types in terms of costs per kilometer. At a configuration of 58 kWh, the maximum range of the analyzed electric vehicle is reduced by 22 km when using SIB cells instead of NMC. Due to spatial constraints resulting from lower volumetric energy densities of SIB cells, their implementation is particularly advantageous in electric vehicles with medium battery capacity. The analysis indicates that when implementing SIBs in electric vehicles, utilizing the maximum possible battery capacity is beneficial, as the low investment costs of these cells favor maximizing range through home charging rather than relying on more expensive public charging infrastructure. This economic advantage is particularly pronounced when low-cost home charging options are available, such as those enabled by photovoltaic systems. Sensitivity analysis of SIB cell properties reveals that gravimetric energy density has a comparably lower impact at the vehicle level. At the same time, specific battery costs significantly influence overall costs, and volumetric energy density substantially affects the packaging space and, thus, the feasible electric vehicle design. From a cost perspective, SIBs represent a promising alternative to conventional LIBs within this use-case analysis, with vehicles in the low and particularly the medium battery capacity range benefiting from this cell technology. This study provides a foundation for researchers to assess innovative technologies and quantify vehicle-level implications. The methodology can be further applied to evaluate the potential of future battery technologies for electric vehicle applications.

## CRediT authorship contribution statement

**Jan Koloch:** Writing – original draft, Software, Methodology, Conceptualization. **Jakob Schneider:** Writing – review & editing, Methodology, Investigation. **Moritz Seidenfus:** Writing – review & editing, Investigation. **Markus Lienkamp:** Writing – review & editing, Supervision, Resources, Funding acquisition.

## Declaration of competing interest

The authors declare that they have no known competing financial interests or personal relationships that could have appeared to influence the work reported in this paper.

## Acknowledgments

The work of J.K. was sponsored by the Federal Ministry for Economic Affairs and Climate Action Germany within the project “Transformations-Hub Scale-up E-Drive” under grant number 16THB0006C. The work of J.S. was sponsored by the Federal Ministry for Economic Affairs and Climate Action Germany within the project “NEFTON” under grant number 01MV21004A. The work of M.S. was funded by the Federal Ministry of Education and Research Germany within the project “STEAM” under grant number 03ZU1105FA. We thank Maksymilian Waldemar Kasperk for supporting the literature review and manuscript revision.

## Data availability

Data will be made available on request.

## References

- [1] P. Plötz, J. Wachsmuth, F. Sprei, T. Gnann, D. Speth, F. Neuner, S. Link, Greenhouse gas emission budgets and policies for zero-Carbon road transport in Europe, *Clim. Policy* 23 (3) (2023) 343–354, <http://dx.doi.org/10.1080/14693062.2023.2185585>.
- [2] H.-W. Schiffer, Treibhausgasneutralität 2045/2050: Verschärfung der nationalen und der europäischen Klimaziele, *Wirtschaftsdienst* 101 (8) (2021) 638–644, <http://dx.doi.org/10.1007/s10273-021-2982-6>.
- [3] Umweltbundesamt, Treibhausgas-emissionen in der Europäischen union, 2024, URL <https://www.umweltbundesamt.de/daten/klima/treibhausgas-emissionen-in-der-europaeischen-union>.
- [4] Umweltbundesamt, Treibhausgas-emissionen in deutschland, 2024, URL <https://www.umweltbundesamt.de/daten/klima/treibhausgas-emissionen-in-deutschland>.
- [5] J. Dornoff, F. Rodríguez, Euro 7: The new emission standard for light- and heavy-duty vehicles in the European Union, 2024, URL <https://theicet.org/publication/euro-7-emission-standard-ldv-hdv-eu-mar24/>.
- [6] Council of the European Union, Interinstitutional file: 2022/0365(COD): Regulation on type-approval of motor vehicles and engines and of systems, components and separate technical units intended for such vehicles, with respect to their emissions and battery durability (Euro 7) - Analysis of the final compromise text with a view to agreement, 2023, URL [https://eur-lex.europa.eu/procedure/EN/2022\\_365](https://eur-lex.europa.eu/procedure/EN/2022_365).
- [7] C. Morgan, J. Goodwin, Impact of the proposed Euro 7 Regulations on exhaust aftertreatment system design, *Johns. Matthey Technol. Rev.* 67 (2) (2023) 239–245, <http://dx.doi.org/10.1595/205651323X16805977899699>.
- [8] Bundesministerium für Umwelt, Naturschutz und nukleare Sicherheit, Das System der CO<sub>2</sub>-Flottengrenzwerte für Pkw und leichte Nutzfahrzeuge, Informationsspapier, Berlin, 2020, p. 10, URL [https://www.bmv.de/fileadmin/Daten\\_BMU/Download\\_PDF/Luft/zusammenfassung\\_co2\\_flottengrenzwerte.pdf](https://www.bmv.de/fileadmin/Daten_BMU/Download_PDF/Luft/zusammenfassung_co2_flottengrenzwerte.pdf).
- [9] A. Pamidimukkala, S. Kermanshachi, J.M. Rosenberger, G. Hladik, Barriers and motivators to the adoption of electric vehicles: A global review, *Green Energy Intell. Transp.* 3 (2) (2024) 100153, <http://dx.doi.org/10.1016/j.geits.2024.100153>.
- [10] A. König, L. Nicoletti, D. Schröder, S. Wolff, A. Waclaw, M. Lienkamp, An overview of parameter and cost for battery electric vehicles, *World Electr. Veh. J.* 12 (1) (2021) 21, <http://dx.doi.org/10.3390/wevj12010021>.
- [11] R.R. Kumar, K. Alok, Adoption of electric vehicle: A literature review and prospects for sustainability, *J. Clean. Prod.* 253 (2020) 119911, <http://dx.doi.org/10.1016/j.jclepro.2019.119911>.
- [12] J. Deng, C. Bae, A. Denlinger, T. Miller, Electric vehicles batteries: Requirements and challenges, *Joule* 4 (3) (2020) 511–515, <http://dx.doi.org/10.1016/j.joule.2020.01.013>.
- [13] P. Dechent, A. Epp, D. Jöst, Y. Preger, P.M. Attia, W. Li, D.U. Sauer, ENPOLITE: Comparing lithium-ion cells across energy, power, lifetime, and temperature, *ACS Energy Lett.* 6 (6) (2021) 2351–2355, <http://dx.doi.org/10.1021/acsenerylett.1c00743>.
- [14] X. Hu, C. Wang, X. Zhu, C. Yao, P. Ghadimi, Trade structure and risk transmission in the international automotive li-ion batteries trade, *Resour. Conserv. Recycl.* 170 (2021) 105591, <http://dx.doi.org/10.1016/j.resconrec.2021.105591>.
- [15] X.-t. Zhao, X.-g. Li, Q. Gao, X.-l. Li, G.-l. Wei, S. Yan, X.-n. Zhu, Y.-g. Ren, Sustainable and efficient recycling strategies for spent lithium iron phosphate batteries: Current status and prospect, *Sep. Purif. Technol.* 359 (2025) 130885, <http://dx.doi.org/10.1016/j.seppur.2024.130885>.
- [16] Y. Zhou, X. Tang, D. Qing, J. Li, H. Wang, Research progress of technology of lithium extraction, *Sep. Purif. Technol.* 359 (2025) 130561, <http://dx.doi.org/10.1016/j.seppur.2024.130561>.
- [17] Nagmani, D. Pahari, P. Verma, S. Puravankara, Are na-ion batteries nearing the energy storage tipping point? – Current status of non-aqueous, aqueous, and solid-sate Na-ion battery technologies for sustainable energy storage, *J. Energy Storage* 56 (2022) 105961, <http://dx.doi.org/10.1016/j.est.2022.105961>.
- [18] C. Delmas, Sodium and sodium–ion batteries: 50 years of research, *Adv. Energy Mater.* 8 (17) (2018) <http://dx.doi.org/10.1002/aenm.201703137>.
- [19] T. Yu, G. Li, Y. Duan, Y. Wu, T. Zhang, X. Zhao, M. Luo, Y. Liu, The research and industrialization progress and prospects of sodium ion battery, *J. Alloys Compd.* 958 (2023) 170486, <http://dx.doi.org/10.1016/j.jallcom.2023.170486>.
- [20] A.N. Singh, M. Islam, A. Meena, M. Faizan, D. Han, C. Bathula, A. Hajibabaei, R. Anand, K.-W. Nam, Unleashing the potential of Sodium–Ion Batteries: Current state and future directions for sustainable energy storage, *Adv. Funct. Mater.* 33 (46) (2023) <http://dx.doi.org/10.1002/adfm.202304617>.
- [21] X. Shu, Y. Li, B. Yang, Q. Wang, K. Puniyawudho, Research on the electrochemical impedance spectroscopy evolution of Sodium–Ion batteries in different states, *Mol. (Basel, Switzerland)* 29 (20) (2024) <http://dx.doi.org/10.3390/molecules29204963>.
- [22] A. Rudola, R. Sayers, C.J. Wright, J. Barker, Opportunities for moderate-range electric vehicles using sustainable sodium-ion batteries, *Nat. Energy* 8 (3) (2023) 215–218, <http://dx.doi.org/10.1038/s41560-023-01215-w>.
- [23] B. Tang, X. Yu, Y. Gao, S.-H. Bo, Z. Zhou, Positioning solid-state sodium batteries in future transportation and energy storage, *Sci. Bull.* 67 (21) (2022) 2149–2153, <http://dx.doi.org/10.1016/j.scib.2022.10.014>.
- [24] Northvolt, Sodium-ion Cells, 2024, URL <https://northvolt.com/products/cells/sodium-ion/>.
- [25] C. Randall, First sodium-ion battery EVs go into serial production in China, 2024, URL <https://www.electrive.com/2024/01/02/first-sodium-ion-battery-evs-go-into-serial-production-in-china/>.
- [26] Jet Sanchez, BYD breaks ground on world's largest sodium-ion battery plant, 2024, URL <https://www.drivencarguide.co.nz/news/byd-breaks-ground-on-worlds-largest-sodium-ion-battery-plant/>.
- [27] Peter Johnson, Volkswagen-backed EV maker rolls out first sodium-ion battery powered electric car, 2023, URL <https://electrek.co/2023/12/27/volkswagen-backed-ev-maker-first-sodium-ion-battery-electric-car/>.
- [28] O. Teichert, S. Link, J. Schneider, S. Wolff, M. Lienkamp, Techno-economic cell selection for battery-electric long-haul trucks, *ETransportation* 16 (2023) 100225, <http://dx.doi.org/10.1016/j.etrans.2022.100225>.
- [29] J. Schneider, O. Teichert, M. Zähringer, K. Götz, M. Lienkamp, Spoilt for choice: User-centric choice of battery size and chemistry for battery-electric long-haul trucks, *Energies* 17 (1) (2024) 158, <http://dx.doi.org/10.3390/en17010158>.
- [30] J. Schneider, S. Wolff, M. Seidenfus, M. Lienkamp, Sizing up sustainability: Influence of battery size and cell chemistry on battery-electric trucks' life-cycle carbon emissions, *E-Prime - Adv. Electr. Eng. Electron. Energy* 9 (2024) 100656, <http://dx.doi.org/10.1016/j.prime.2024.100656>.
- [31] S. Link, M. Stephan, L. Weymann, T. Hettesheimer, Techno-economic suitability of batteries for different mobile applications—A cell selection methodology based on cost parity pricing, *World Electr. Veh. J.* 15 (9) (2024) 401, <http://dx.doi.org/10.3390/wevj15090401>.
- [32] S. Hasselwander, M. Meyer, I. Österle, Techno-economic analysis of different battery cell chemistries for the passenger vehicle market, *Batteries* 9 (7) (2023) 379, <http://dx.doi.org/10.3390/batteries9070379>.
- [33] A. König, L. Nicoletti, S. Kalt, K. Müller, A. Koch, M. Lienkamp, An open-source modular quasi-static longitudinal simulation for full electric vehicles, in: 2020 Fifteenth International Conference on Ecological Vehicles and Renewable Energies, EVER, IEEE, 2020, pp. 1–9, <http://dx.doi.org/10.1109/EVER48776.2020.9242981>.
- [34] ADAC, VW ID.3 im ADAC autokatalog, 2024, URL <https://www.adac.de/rundums-fahrzeug/autokatalog/marken-modelle/vw/id3/>.
- [35] N. Wassiliadis, M. Steinräter, M. Schreiber, P. Rosner, L. Nicoletti, F. Schmid, M. Ank, O. Teichert, L. Wildfeuer, J. Schneider, A. Koch, A. König, A. Glatz, J. Gandlgruber, T. Kröger, X. Lin, M. Lienkamp, Quantifying the state of the art of electric powertrains in battery electric vehicles: Range, efficiency, and lifetime from component to system level of the Volkswagen ID.3, *ETransportation* 12 (2022) 100167, <http://dx.doi.org/10.1016/j.etrans.2022.100167>.
- [36] L. Schlotter, Empirical analysis of the depreciation of electric vehicles compared to gasoline vehicles, *Transp. Policy* 126 (2022) 268–279, <http://dx.doi.org/10.1016/j.tranpol.2022.07.021>.
- [37] Z. Liu, J. Song, J. Kubal, N. Susarla, K.W. Knehr, E. Islam, P. Nelson, S. Ahmed, Comparing total cost of ownership of battery electric vehicles and internal combustion engine vehicles, *Energy Policy* 158 (2021) 112564, <http://dx.doi.org/10.1016/j.enpol.2021.112564>.
- [38] N. Parker, H.L. Breetz, D. Salon, M.W. Conway, J. Williams, M. Patterson, Who saves money buying electric vehicles? Heterogeneity in total cost of ownership, *Transp. Res. D: Transp. Environ.* 96 (2021) 102893, <http://dx.doi.org/10.1016/j.trd.2021.102893>.
- [39] W. Mei, Z. Cheng, L. Wang, A. Teng, Z. Li, K. Jin, J. Sun, Q. Wang, Thermal hazard comparison and assessment of Li-ion battery and Na-ion battery, *J. Energy Chem.* (2024) <http://dx.doi.org/10.1016/j.jchem.2024.10.036>.
- [40] H. Kim, Sodium-Ion battery: Can it compete with Li-Ion? *ACS Mater.* Au 3 (6) (2023) 571–575, <http://dx.doi.org/10.1021/acsmaterialsau.3c00049>.
- [41] Verivox, Strompreisentwicklung 2014–2024, 2024, URL <https://www.verivox.de/strom/strompreisentwicklung/>.
- [42] ADAC, Ladetarife für elektroautos: Anbieter und Kosten im Vergleich, 2024, URL <https://www.adac.de/rund-ums-fahrzeug/elektromobilitaet/laden/elektroauto-ladesaeulen-strompreise/>.
- [43] C. Xu, Q. Dai, L. Gaines, M. Hu, A. Tukker, B. Steubing, Future material demand for automotive lithium-based batteries, *Commun. Mater.* 1 (1) (2020) <http://dx.doi.org/10.1038/s43246-020-00095-x>.
- [44] B. Dalla Chiara, F. Defflorio, M. Pellicelli, L. Castello, M. Eid, Perspectives on electrification for the automotive sector: A critical review of average daily distances by light-duty vehicles, required range, and economic outcomes, *Sustainability* 11 (20) (2019) 5784, <http://dx.doi.org/10.3390/su11205784>.
- [45] X. Hao, H. Wang, Z. Lin, M. Ouyang, Seasonal effects on electric vehicle energy consumption and driving range: A case study on personal, taxi, and ridesharing vehicles, *J. Clean. Prod.* 249 (2020) 119403, <http://dx.doi.org/10.1016/j.jclepro.2019.119403>.
- [46] A. Celadon, H. Sun, S. Sun, G. Zhang, Batteries for electric vehicles: Technical advancements, environmental challenges, and market perspectives, *SusMat* 4 (5) (2024) <http://dx.doi.org/10.1002/sus2.234>.

[47] R. Wanison, W.N.H. Syahputra, N. Kammuang-lue, P. Sakulchangsattajai, C. Chaichana, V.U. Shankar, P. Suttakul, Y. Mona, Engineering aspects of sodium-ion battery: An alternative energy device for Lithium-ion batteries, J. Energy Storage 100 (2024) 113497, <http://dx.doi.org/10.1016/j.est.2024.113497>.



**Jan Koloch** received a bachelor's in engineering science and a master's in automotive engineering from the Technical University of Munich (TUM). He is currently pursuing a Ph.D. degree with the Institute of Automotive Technology at TUM. His research focuses on innovative battery technologies and their influence on the system design of battery-electric vehicles.



**Jakob Schneider** received a bachelor's in mechanical engineering and a master's in automotive engineering from the Technical University of Munich (TUM). He is currently pursuing a Ph.D. degree with the Institute of Automotive Technology at TUM. His research focuses on battery sizing, cell chemistry selection, the influence of future battery technologies and fast charging for heavy-duty vehicles.



**Moritz Seidenfus** received a bachelor's in mechanical engineering and a master's in automotive engineering from the Technical University of Munich (TUM). He is currently pursuing a Ph.D. degree with the Institute of Automotive Technology at TUM. His research focuses sustainability metrics for large scale mobility systems and parametric Life-cycle assessment.



**Markus Lienkamp** is conducting research in the area of electro-mobility with the objective of developing new vehicle concepts. He is professor of the Institute of Automotive Technology at Technical University of Munich (TUM). After studying mechanical engineering at TU Darmstadt and Cornell University, he obtained his doctorate at TU Darmstadt (1995). He worked at Volkswagen as part of an international trainee program and took part in a joint venture between Ford and Volkswagen in Portugal. Returning to Germany, he led the brake testing department in the VW commercial vehicle development section in Wolfsburg. He later became head of the "Electronics and Vehicle" research department in Volkswagen AG's Group Research division. His main priorities were advanced driver assistance systems and vehicle concepts for electro-mobility. Prof. Lienkamp is heading the Chair of Automotive Technology at TUM since November 2009.